

# Cosmological Neutrino Background Revisited

Nickolay Y. Gnedin

Department of Astronomy, University of California, Berkeley, CA 94720; gnedin@astron.berkeley.edu

and

Oleg Y. Gnedin

Princeton University Observatory, Princeton, NJ 08544; ognedin@astro.princeton.edu

## ABSTRACT

We solve the Boltzmann equation for cosmological neutrinos around the epoch of the electron-positron annihilation in order to verify the freeze-out approximation and to compute accurately the cosmological neutrino distribution function. We find the radiation energy density to be about 0.6% higher than the one predicted by the freeze-out approximation. As a result, the spectrum of the Cosmic Microwave Background anisotropies changes by  $\sim 0.6 - 1\%$ , depending on the angular scale, and the amplitude of the mass fluctuations on scales below about  $100 h^{-1} \text{Mpc}$  decreases by about 0.3-0.5%.

## 1. Introduction

Anisotropies in the Cosmic Microwave Background (CMB) provide a powerful tool to probe the cosmological parameters (Hu, Sugiyama & Silk 1997). The results of four-year work of the COBE satellite (Bennett et al. 1996) allow us to determine the power spectrum of the CMB anisotropies to an accuracy of 7%, but with relatively poor angular resolution,  $\theta_{\text{FWHM}} \approx 7^\circ$ . New planned satellite missions, MAP (Bennett et al. 1997) and Planck (Bersanelli et al. 1997), will achieve an accuracy of better than 1% in the power spectrum with the sub-degree resolution (Bond, Efstathiou & Tegmark 1997; Zaldarriaga, Spergel & Seljak 1997). In turn, we need to bring the theoretical models to the same level of accuracy.

In the standard cosmological model, after the epoch of the Big Bang Nucleosynthesis the relativistic particles include photons and the three species of neutrinos (Kolb & Turner 1990; Peebles 1993). While the abundance of photons is directly measured from the CMB observations, the abundance of primordial neutrinos can only be assessed theoretically. The standard way to perform such a calculation is to use the so called freeze-out approximation, which assumes that neutrinos decouple instantaneously from the rest of the universe at temperature of about 4 MeV. Then the distribution function of all three neutrino species retains the Fermi-Dirac form with the only parameter, the neutrino temperature, uniquely tied to the observed CMB temperature.

However, even after decoupling the high-energy neutrinos still interact, albeit slowly, with the electron-positron plasma, contrary to the basic assumption of the freeze-out approximation. This interaction leads to some of the photon energy being transferred into neutrinos. But because it is the photon energy density that is directly measured, the total energy density of the universe in the relativistic species *relative* to the energy density in photons (which is measured observationally to about 0.3% accuracy) will be somewhat higher than the one predicted by the freeze-out approximation.

Several previous attempts have been made to compute cosmological neutrino decoupling in greater detail, but still assuming that neutrino distribution functions have Maxwellian form (Dicus et al. 1982;

Herrera & Hacyan 1989; Raha & Mitra 1991; Dolgov & Fukugita 1992), with the most comprehensive study given by Dodelson & Turner (1992). Recently, two more papers have addressed this problem with the full account for the Fermi-Dirac form of the neutrino distribution functions (Hannestad & Madsen 1995; Dolgov, Hansen, & Semikoz 1997). Both those papers, however, have not achieved the desired level of accuracy (about  $10^{-4}$ , which is equivalent to a 1% accuracy in a 1% correction to the freeze-out approximation) in numerical calculation due to the complexity of the problem: solving the full Boltzmann equation presents a three dimensional problem, which is at the very edge of modern computing capabilities. As a result, the previous papers have only been able to cover slightly more than two decades in the neutrino momentum, which is insufficient to compute the asymptotic behavior of the neutrino distribution function in the limits of very small or very large values of the neutrino momentum.

In this paper we complete the calculation of cosmological neutrino decoupling using an extensive calculation on a parallel supercomputer, placing special emphasis on achieving the complete numerical convergence, and covering over seven decades in the neutrino momentum.

The paper is composed in the following way: we review the freeze-out approximation in §2; we derive and solve the Boltzmann equations for all three neutrino species in §3. In Section 5, we present our results for the neutrino energy density and compare them to the freeze-out approximation. We also obtain accurate distribution functions for cosmological neutrinos.

## 2. The Freeze-out Approximation for the Cosmological Neutrino Background

In the standard cosmological model, after the muon pair annihilation at  $T \sim 100$  MeV, the universe is filled with photons, electron-positron pairs, three species of neutrinos, and nucleons (protons and neutrons). The number density of nucleons is about  $10^{-9}$  of the number density of photons, and the former contribute only about  $10^{-6}$  of the total energy density of the universe. There may also exist particles constituting cold dark matter but these particles are assumed (a) to be nonrelativistic, contributing no more than about  $10^{-5}$  of the total energy density; and (b) not to interact with the rest of the matter in the universe. Thus, the energy density of the universe is determined by the photons, electrons, positrons, and neutrinos.

These particles interact with each other. Photons interact with electron-positron pairs via pair creation/annihilation, and this process is so efficient at temperatures above 0.1 MeV that to a very high accuracy both photons and electron-positron pairs are in thermal equilibrium. Electron neutrinos interact with electron-positron pairs via the following reactions:

$$\nu_e + \bar{\nu}_e \leftrightarrow e^- + e^+, \quad (1)$$

and

$$e^\pm + \nu_e \leftrightarrow e^\pm + \nu_e. \quad (2)$$

Muon and tau neutrinos also interact with their respective leptons (muons and tau leptons), but since both muons and tau leptons have annihilated long before  $T \sim 10$  MeV, their abundances are small, and the reactions like

$$\nu_\mu + \bar{\nu}_\mu \leftrightarrow \mu^- + \mu^+ \quad (3)$$

are strongly suppressed. Thus, the main channel of interactions for muon and tau neutrino is via electron-positron pair creation and electron/positron scattering:

$$\nu + \bar{\nu} \leftrightarrow e^- + e^+, \quad (4)$$

and

$$e^\pm + \nu \leftrightarrow e^\pm + \nu, \quad (5)$$

where the symbol  $\nu$  stands for any type of neutrino. The reactions (4,5) for muon and tau neutrinos are somewhat slower than respective reactions for electron neutrinos (1,2). In addition, there are reactions between different species of neutrinos:

$$\nu_i + \nu_j \leftrightarrow \nu_k + \nu_l, \quad (6)$$

where indices  $i, j, k$ , and  $l$  denote electron, muon, or tau neutrino. The full set of relevant reactions is given in Table 1.

The standard way to compute the thermal history of the universe just before and after the electron-positron annihilation is to assume that neutrinos decouple instantaneously when the rate of the reaction equals the expansion rate:

$$\langle v\sigma \rangle n_\nu = H, \quad (7)$$

where  $H$  is the Hubble constant. For electron neutrinos participating in reaction (4) this happens at  $T \sim 4\text{MeV}$ , and for muon and tau neutrinos this happens at a slightly higher temperature. Assuming that electrons and positrons do not decouple from photons at  $T \sim 4\text{MeV}$ , we can compute the present day neutrino temperature by merely counting the degrees of freedom before and after the electron-positron annihilation.

Before the electron-positron annihilation, the entropy of the photons and electron-positron pairs in thermal equilibrium within the volume  $V$  is:

$$S = \frac{4}{3} \frac{\rho}{T} V = \frac{4}{3} a_R T^3 V \left( 1 + \frac{7}{8} + \frac{7}{8} \right) = \frac{11}{3} a_R T^3 V, \quad (8)$$

where  $a_R$  is the radiation energy density constant. After the annihilation, all this entropy is transferred to the photons and thus

$$S = \frac{4}{3} a_R T^3 V. \quad (9)$$

By combining equations (8) and (9), and recalling that the volume increases as  $V \sim a^3$  in the expanding universe, where  $a$  is the cosmological scale factor, we obtain:

$$(aT)_{\text{before}} = \left( \frac{4}{11} \right)^{1/3} (aT)_{\text{after}}. \quad (10)$$

Since all three neutrino species decoupled *before* the electron-positron annihilation, their current temperature is

$$T_{0,\nu} = (aT)_{\text{before}},$$

while the photon current temperature is

$$T_{0,\gamma} = (aT)_{\text{after}}.$$

Here subscript 0 refers to the current epoch,  $a = 1$ . Thus, we find the standard result of the freeze-out approximation,

$$T_{0,\nu} = \left( \frac{4}{11} \right)^{1/3} T_{0,\gamma}. \quad (11)$$

Thus, the radiation energy density at the current epoch is

$$\epsilon_R = \left[ 1 + \frac{21}{8} \left( \frac{4}{11} \right)^{4/3} \right] a_R T_{0,\gamma}^4 = 1.6813 a_R T_{0,\gamma}^4. \quad (12)$$

### 3. Neutrino Kinetics in the Expanding Universe

The Boltzmann equation for neutrinos in the expanding universe is (Kolb & Turner 1990):

$$E_\nu \frac{\partial f_\nu}{\partial t} - Hq^2 \frac{\partial f_\nu}{\partial E_\nu} = \mathcal{C}[f_\nu], \quad (13)$$

where  $f_\nu(q, t)$  is the neutrino distribution function,  $E_\nu$  is the neutrino energy ( $E_\nu = q$  since the neutrino mass, even if it exists, is assumed to be much smaller than our characteristic energy scale,  $\sim \text{MeV}$ ), and  $\mathcal{C}[f_\nu]$  is the collisional integral. Hereafter we use units in which  $\hbar = c = 1$ . In the case of neutrinos interacting with the electron-positron pairs and other neutrino species via annihilation and scattering reactions (eqs. 4,5,6), the collisional integral is (Hannestad & Madsen 1995)

$$\mathcal{C}[f_\nu] = \sum \frac{1}{2(2\pi)^5} \int \frac{d^3p_2}{2E_2} \frac{d^3p_3}{2E_3} \frac{d^3p_4}{2E_4} \Lambda(f_1, f_2, f_3, f_4) M^2 \delta^4(\bar{p}_1 + \bar{p}_2 - \bar{p}_3 - \bar{p}_4), \quad (14)$$

where  $p_1 \equiv q$ ,  $f_1 \equiv f_\nu$ ,

$$\Lambda(f_1, f_2, f_3, f_4) \equiv f_4 f_3 (1 - f_2)(1 - f_1) - f_1 f_2 (1 - f_3)(1 - f_4),$$

$M^2$  is the matrix element squared and summed over initial and final spin states,  $\bar{p}_i$  are four-momenta of the incoming (1,2) and outgoing (3,4) particles, and the sum is taken over all of the reactions involving  $f_1$ .

The list of all neutrino reactions is presented in Table 1, along with the respective matrix elements (Hannestad & Madsen 1995). Indices  $i, j, k$  run over electron, muon, and tau neutrino, with the exception that  $j \neq i$ . The factor  $G_F$  is the Fermi coupling constant, and coefficients  $C_V$  and  $C_A$  for different types of neutrinos are given by the following equations (for example, Kaminker et al. 1992):

$$\begin{aligned} C_V(\nu_e) &= 2 \sin^2 \Theta_W + \frac{1}{2}, & C_A(\nu_e) &= \frac{1}{2}, \\ C_V(\nu_\mu, \nu_\tau) &= 2 \sin^2 \Theta_W - \frac{1}{2}, & C_A(\nu_\mu, \nu_\tau) &= -\frac{1}{2}, \end{aligned}$$

where  $\Theta_W$  is the Weinberg angle, and we adopt  $\sin^2 \Theta_W = 0.23$ .

Quantities  $Q_i$  are defined as follows:

$$Q_1 = (\bar{p}_1 \cdot \bar{p}_2)(\bar{p}_3 \cdot \bar{p}_4),$$

Table 1: Neutrino Reactions

Reaction	$M^2$
$\nu_i + \bar{\nu}_i \rightarrow e^- + e^+$	$32G_F^2 [(C_V + C_A)^2 Q_3 + (C_V - C_A)^2 Q_2 + (C_V^2 - C_A^2) Q_4]$
$\nu_i + e^- \rightarrow \nu_i + e^-$	$32G_F^2 [(C_V + C_A)^2 Q_1 + (C_V - C_A)^2 Q_3 - (C_V^2 - C_A^2) Q_5]$
$\nu_i + e^+ \rightarrow \nu_i + e^+$	$32G_F^2 [(C_V + C_A)^2 Q_3 + (C_V - C_A)^2 Q_1 - (C_V^2 - C_A^2) Q_5]$
$\nu_i + \bar{\nu}_i \rightarrow \nu_i + \bar{\nu}_i$	$128G_F^2 Q_3$
$\nu_i + \bar{\nu}_i \rightarrow \nu_j + \bar{\nu}_j$	$32G_F^2 Q_3$
$\nu_i + \bar{\nu}_j \rightarrow \nu_i + \bar{\nu}_j$	$32G_F^2 Q_3$
$\nu_i + \nu_k \rightarrow \nu_i + \nu_k$	$32G_F^2 Q_1$

$$\begin{aligned}
Q_2 &= (\bar{p}_1 \cdot \bar{p}_3)(\bar{p}_2 \cdot \bar{p}_4), \\
Q_3 &= (\bar{p}_1 \cdot \bar{p}_4)(\bar{p}_2 \cdot \bar{p}_3), \\
Q_4 &= m^2(\bar{p}_1 \cdot \bar{p}_2), \\
Q_5 &= m^2(\bar{p}_1 \cdot \bar{p}_3),
\end{aligned} \tag{15}$$

where  $m$  is the electron mass. As has been shown by Hannestad & Madsen (1995), integrals over  $d^3p_4$  and over angles in  $d^3p_2$  and  $d^3p_3$  can be computed analytically, yielding

$$\mathcal{C}[f_\nu] = \sum \frac{1}{2(2\pi)^5} \int \frac{p_2^2 dp_2}{2E_2} \frac{p_3^2 dp_3}{2E_3} \Lambda(f_1, f_2, f_3, f_4) F(p_1, p_2, p_3). \tag{16}$$

Factors  $F(p_1, p_2, p_3)$  are very complicated, and in order to minimize the possibility of an error, we have used *Mathematica* software package to perform the calculations. The resultant formulas are too large to be presented here, but the original *Mathematica* code which generates all the relevant expressions and the FORTRAN source code are available from the authors upon request.

In order to solve for the evolution of the neutrino distribution functions  $f_\nu(\zeta)$ , we need to add the equations describing the evolution of the scale factor and the energy density of the universe:

$$\frac{da}{dt} = \left( \frac{8\pi G}{3} \rho \right)^{1/2} a, \tag{17}$$

and

$$\frac{d\rho}{dt} = -3H(\rho + p), \tag{18}$$

where  $\rho$  and  $p$  are the energy density and the pressure, respectively:

$$\begin{aligned}
\rho(T) &= \frac{T^4}{\pi^2} \left[ 2C_{1/2}(\lambda) + \frac{\pi^4}{15} \right] + \rho_\nu, \\
p(T) &= \frac{T^4}{\pi^2} \left[ \frac{2}{3} (C_{1/2}(\lambda) - \lambda^2 C_{-1/2}(\lambda)) + \frac{\pi^4}{45} \right] + \frac{\rho_\nu}{3},
\end{aligned}$$

where  $\lambda \equiv m/T$  and the functions  $C_n(\lambda)$  are defined as

$$C_n(\lambda) \equiv \int_\lambda^\infty \frac{\sqrt{x^2 - \lambda^2} x^{2n+1} dx}{e^x + 1}.$$

Here  $\rho_\nu$  is the energy density in the three neutrino species,

$$\rho_\nu = \frac{1}{\pi^2} \int_0^\infty q^3 [f_{\nu_e}(q) + f_{\nu_\mu}(q) + f_{\nu_\tau}(q)] dq.$$

We also note that since the coefficients  $C_V$  and  $C_A$  are the same for muon and tau neutrino, their distribution functions are equal.

#### 4. Numerical Issues

Equation (13) can now be integrated numerically for each neutrino species, along with equations (17) and (18). In order to eliminate the derivative with respect to the neutrino momentum in (13), we switch to

the comoving momentum  $\zeta = qa$ . We lay out the neutrino distribution function on a logarithmically spaced mesh in the range  $10^{-5.5} \leq q/T \leq 10^{1.7}$  with 40 points per decade (289 points altogether). By appropriately changing the limits and sampling of the momentum mesh, we have verified that such a discretization offers a fully convergent solution to an accuracy of better than  $10^{-4}$ . After this procedure, equation (13) becomes a system of coupled ordinary differential equations. We use double precision and we find that, due to the specifics of numerical error propagation, we need to set the relative accuracy of integration to  $10^{-7}$ . We begin our integration at  $T = 10 \text{ MeV}$  and stop it at  $T = 10^{-3} \text{ MeV}$ , and which has been verified to be sufficient to maintain the desired accuracy.

The resultant ordinary differential equations are stiff and solving them offers a considerable computational challenge. In addition, these equations are sufficiently complicated so that it is virtually impossible to compute the full Jacobian of the system of equations, which is needed in order to use a standard method for stiff problems. Therefore, we develop a special numerical scheme presented in the Appendix, which can handle stiff equations of the Boltzmann type but does not require computing the full Jacobian. Our scheme gives us a gain of a factor of 20 to 60 as compared to the standard fifth order adaptive Runge-Kutta method.

Finally, we note that the most time consuming part, calculating the collisional integral, can be done every efficiently in parallel. Our final computation has been performed on the NCSA Power Challenge Array with 12 R10K processors and has consumed about 960 processor-hours.

## 5. Results and Discussion

The main results of our calculations are the number density and the energy density of all three neutrino species at the current epoch relative to those of photons. These results are presented in Table 2. For comparison, we also give the respective numbers computed in the freeze-out approximation. All these numbers are accurate to the last decimal place shown. The most important quantity, the total radiation energy density in the universe, differs from the freeze-out approximation by only 0.6%.

Another way of presenting this difference is the effective number of neutrino species,  $N_{\text{eff}}$ . We can rewrite the expression for the energy density of the universe as

$$\epsilon_R = \left[ 1 + N_{\text{eff}} \frac{7}{8} \left( \frac{4}{11} \right)^{4/3} \right] a_R T_{0,\gamma}^4, \quad (19)$$

Table 2: Main Results

Quantity	Exact value	Value from the freeze-out approximation
$(aT)_{\text{before}}$	$0.7151(aT)_{\text{after}}$	$0.7138(aT)_{\text{after}}$
$\epsilon_R$	$1.6915 a_R T_{0,\gamma}^4$	$1.6813 a_R T_{0,\gamma}^4$
$\epsilon_{\nu_e}$	$0.2313 a_R T_{0,\gamma}^4$	$0.2271 a_R T_{0,\gamma}^4$
$\epsilon_{\nu_\mu}$	$0.2301 a_R T_{0,\gamma}^4$	$0.2271 a_R T_{0,\gamma}^4$
$\epsilon_{\nu_\tau}$	$0.2301 a_R T_{0,\gamma}^4$	$0.2271 a_R T_{0,\gamma}^4$
$n_{\nu_e}$	$0.2760 n_\gamma$	$0.2727 n_\gamma$
$n_{\nu_\mu}$	$0.2752 n_\gamma$	$0.2727 n_\gamma$
$n_{\nu_\tau}$	$0.2752 n_\gamma$	$0.2727 n_\gamma$

where in the freeze-out approximation  $N_{\text{eff}} = 3$ . From Table 2 we obtain:

$$N_{\text{eff}} = 3.045.$$

This number does not, of course, mean that there are more than 3 species of neutrinos; it is simply a number that should be used in the freeze-out approximation to reproduce the exact result. But since most of the previously obtained results and existing numerical codes are based on the freeze-out approximation, it is convenient to use  $N_{\text{eff}}$ : one simply has to use 3.045 instead of 3.0 in every place in the code where the neutrino energy density is computed.

We note here that we find a somewhat larger effect than both Hannestad & Madsen (1995) and Dolgov et al. (1997), who found  $N_{\text{eff}} = 3.030$  and  $N_{\text{eff}} = 3.025$  respectively. We attribute this difference to the higher accuracy of our calculation and the lack of numerical convergence in the previous work (the latter is particularly apparent in Table 3 of Dolgov et al. 1997 paper).

We can also characterize the final neutrino distribution function. Let us introduce the effective neutrino temperature,  $T_{\text{eff}}$  as

$$f_{\nu}(q) \equiv \frac{1}{e^{q/T_{\text{eff}}} + 1}. \quad (20)$$

Since the neutrino distribution function is not of the Fermi-Dirac form any more,  $T_{\text{eff}}$  is a function of the neutrino momentum  $q$ . Figure 1 shows the deviation of the effective temperature at the current epoch,  $T_{0,\text{eff}}$ , from the freeze-out approximation,  $T_{0,\nu}$  (eq. 11), as a function of  $q/T$  (this ratio is independent of time after electron-positron annihilation). For the high neutrino momenta, the effective neutrino temperature asymptotically approaches the photon temperature, because the high-energy neutrinos can efficiently interact with the electrons via pair creation even after annihilation,

$$T_{\text{eff}} \rightarrow T \quad \text{for } q \rightarrow \infty.$$

For the low momenta,  $q \ll T$ , neutrino interactions with electrons and positrons are suppressed as  $q^2$ , and do not affect the evolution of the distribution function. However, the rate of neutrino-neutrino interactions is proportional to the first power of the momentum  $q$ . Thus, in the limit of small momenta,

$$\frac{\partial f_{\nu}(q)}{\partial t} = \frac{q}{T_{\text{eff}}^2(0)} \frac{dT_{\text{eff}}(0)}{dt} \propto q,$$

and we find that

$$T_{\text{eff}} \rightarrow \text{const} \quad \text{for } q \rightarrow 0.$$

The value of the constant is  $0.99941T_{0,\nu}$  for electron neutrinos and  $0.99897T_{0,\nu}$  for muon and tau neutrinos.

Our results have two immediate cosmological implications. First, the change in the radiation energy density of the universe will affect the spectrum of CMB anisotropies at about 0.6% level just behind the first acoustic peak,  $l \sim 300$ , and at about 1% level at the damping scale,  $l \sim 1000$  (Hu et al. 1995). If more than 1% accuracy is required in calculating the CMB anisotropies, equation (19) should be used.

Second, the change in the radiation energy density of the universe affects the evolution of linear density fluctuations on galactic and subgalactic scales. We have computed the matter transfer function using *COSMICS* package (Bertschinger 1995) and we find that for a cosmological model with  $\Omega_0 = 1$ ,  $h = 0.5$ , and  $\Omega_b = 0.05$ , the rms density fluctuation at  $8h^{-1}$  Mpc scale,  $\sigma_8$ , decreases by 0.34%, and the rms density fluctuation on  $100h^{-1}$  kpc scale decreases by 0.47%. These changes are however too small to be of any interest in the foreseeable future.

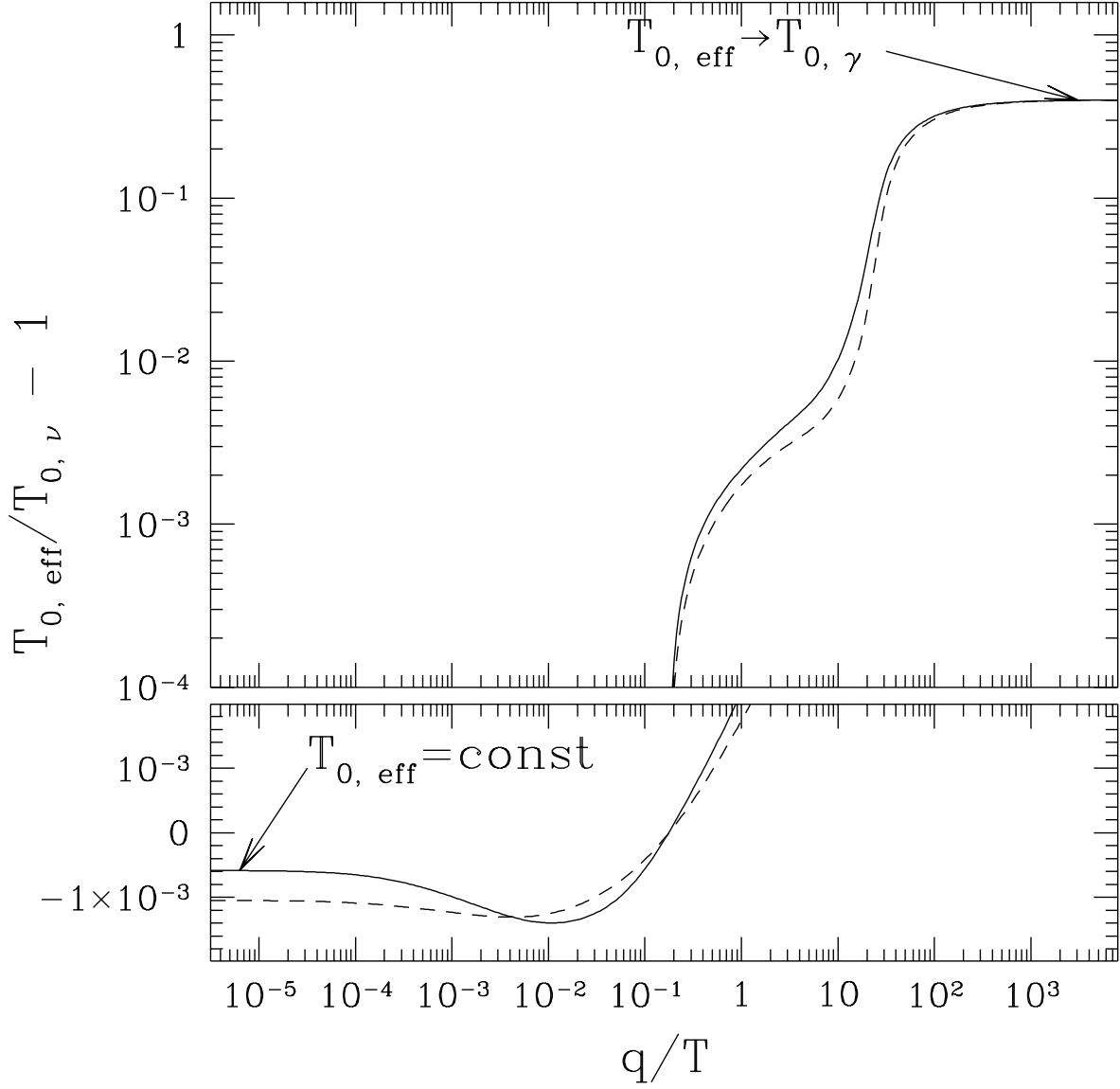


Fig. 1.— The fractional difference between the effective neutrino temperature and its value in the freeze-out approximation, as a function of the neutrino momentum,  $q$ . Solid line is for the electron neutrino temperature, and dashed line is for the muon and tau neutrino temperatures.

In addition, neutrino decoupling affects primordial helium production. However, Dodelson & Turner (1992) showed that the net change in the primordial helium abundance is virtually unobservable due to cancellation of two competing effects: one is the higher expansion rate, which leads to a higher helium abundance, and the other is the faster neutron decay rate, which leads to a lower helium abundance. A small change in the neutrino number density will produce a small change in the massive neutrino mass density (Hannestad & Madsen 1995), but this change is again too small to be of any practical interest.

Thus, we conclude that only in computing the CMB anisotropies one may need to worry about accurate calculation of neutrino decoupling; otherwise, the effect is negligibly small.

In addition, we note here that our calculations confirm the validity of the freeze-out approximation. If the accuracy of a few percent is sufficient, one can safely use the freeze-out approximation to compute any property of cosmological neutrinos.

We are grateful to D. G. Yakovlev and D. Spergel for valuable comments. N. G. was supported by the UC Berkeley grant 1-443839-07427. Calculations were performed on the NCSA Power Challenge Array under the grant AST-960015N.

### A. Numerical Method

In this paper we are dealing with a particular kind of an ordinary differential equation that can be presented in the following form:

$$\frac{dy}{dt} = f(y) \equiv w(y) - k(y)y, \tag{A1}$$

where both  $w$  and  $k$  are slow functions of  $y$ , but not of  $t$ , and  $k$  is positive. This equation is stiff, and a numerical method which does not handle stiff equations requires a time step  $\Delta t$  such that

$$k\Delta t \ll 1.$$

Numerical methods that can deal with stiff equations usually have a much less stringent restriction on the time step,

$$\left| \frac{\partial w}{\partial y} \right| \Delta t \ll 1,$$

and, because  $w$  is a slow function of  $y$ , we assume that

$$\left| \frac{\partial w}{\partial y} \right| \ll k.$$

However, standard techniques for stiff equations require computing the full Jacobian,

$$J = \frac{\partial w}{\partial y} - \frac{\partial k}{\partial y}y - k.$$

In our case this quantity is very difficult to compute, because  $w$  is an integral over  $y$  and numerical evaluation of the integral involves nontrivial interpolation.

We therefore proceed differently, and design a numerical scheme which involves only a partial Jacobian,

$$\hat{J} \equiv -k,$$

which can be computed simultaneously with the r.h.s. of equation (A1) at no extra cost.

Additional advantage of using the partial Jacobian  $\hat{J}$  instead of the full Jacobian  $J$  is that for a system of equations, the partial Jacobian is a diagonal matrix, which can be inverted much faster than the full Jacobian, which is usually a general matrix.

However, we cannot simply take a standard numerical scheme and replace the full Jacobian with the partial one, because the different orders of the numerical error will not cancel out in this case. Thus, we need to design a special scheme which will assure the proper cancellation of the numerical error up to a given order.

The numerical scheme to update  $y$  from  $y = y_0$  to  $y = y_1$  in a time interval  $h$  is constructed as follows:

$$\begin{aligned}
 g_1 &= \frac{hf(y_0)}{1 + \gamma hk}, \\
 g_2 &= \frac{hf(y_0 + a_{21}g_1) + c_{21}g_1}{1 + \gamma hk}, \\
 g_3 &= \frac{hf(y_0 + a_{31}g_1 + a_{32}g_2) + c_{31}g_1 + c_{32}g_2}{1 + \gamma hk}, \\
 y_1 &= y_0 + b_1g_1 + b_2g_2 + b_3g_3,
 \end{aligned} \tag{A2}$$

where  $\gamma$ ,  $a_i$ ,  $b_i$ , and  $c_i$  are constants. The values for  $\gamma$ ,  $a_{21}$ ,  $a_{31}$ ,  $a_{32}$ , and  $c_{21}$  are given in Table 3.

By varying the rest of the constants, we can construct two numerical schemes: the third order and the second order, respectively. Thus, the difference between  $y_1$  computed in each of the two schemes can serve as an estimate for the numerical error. The respective values of constants are given in Table 4. Again, *Mathematica* was used to compute the values of the constants that give the cancellation of the numerical error up to the required order.

## REFERENCES

- Bennett, C., et al. 1996, ApJ Lett., 464, L1.  
 Bennett, C., et al. 1996, MAP web page, <http://map.gsfc.nasa.gov>  
 Bersanelli, M., et al. 1996, Planck web page,  
<http://astro.estec.esa.nl/SA-general/Projects/Cobras/cobras.html>  
 Bertschinger, E. 1995, astro-ph/9506070

Table 3:

Constant	Value
$\gamma$	0.788675134594812882251
$a_{21}$	1
$a_{31}$	0.56698729810778067662
$a_{32}$	1/4
$c_{21}$	-1.26794919243112270647

- Bond, J. R., Efstathiou, G., & Tegmark, M. 1997, MNRAS, submitted (astro-ph/9702100)
- Dicus, D. A., Kolb, E. W., Gleeson, A. M., Sudarshan, E. C. G., Teplits, V. L., & Turner, M. S. 1982, Phys. Rev. D, 26, 2694
- Dodelson, S., & Turner, M. S. 1992, Phys. Rev. D, 46, 3372
- Dolgov, A. D., & Fukugita, M. 1992, JETP Lett., 56, 123
- Dolgov, A. D., Hansen, S. H., & Semikoz, D. V. 1997, Phys. Lett. B, 407, 12
- Hannestad, S., & Madsen, J. 1995, Phys. Rev. D, 52, 1764
- Herrera, M. A., & Hacyan, S. 1989, ApJ, 336, 539
- Hu, W., Scott, D., Sugiyama, N., & White, M. 1995, Phys. Rev. D, 52, 5498
- Hu, W., Sugiyama, N., & Silk, J. 1997, Nature, 386, 37
- Kaminker, A. D., Levenfish, K. P., Yakovlev, D. G., Amsterdamski, P., & Haensel, P. 1992, Phys. Rev. D, 46, 3256
- Kolb, E. W., & Turner, M. S. 1990, The Early Universe (Addison-Wesley)
- Peebles, P. J. E. 1993, Physical Cosmology (Princeton: Princeton University Press)
- Zaldarriaga, M., Spergel, D. N., & Seljak, U. 1997, ApJ, 488, 1

---

This preprint was prepared with the AAS L<sup>A</sup>T<sub>E</sub>X macros v4.0.

Table 4:

Constant	Third order scheme	Second order scheme
$c_{31}$	-3/2	-3.183012701892219323
$c_{32}$	-1.1830127018922193234	-2.781088913245535264
$b_1$	1.3779915320718537844	1.566987298107780677
$b_2$	0.9553418012614795489	1.038675134594812883
$b_3$	2/3	0.21132486540518711775